

# Benefit of later time point PET imaging of HER3 expression using optimized radiocobalt-labeled affibody molecule

Sara S. Rinne, Charles Dahlsson Leitao, Zahra Saleh-nihad, Bogdan Mitran, Vladimir Tolmachev, Stefan Ståhl, John Löfblom and Anna Orlova

## Supplementary Data

**Table 1.** Biodistribution data for [<sup>68</sup>Ga]Ga-(HE)<sub>3</sub>-Z<sub>HER3</sub>-NODAGA (3 h pi) in BxPC-3 xenografted Balb/c nu/nu mice as %ID and tumor-to-organ ratios.

Organ	% ID/g			Tumor to Organ Ratio		
	<sup>68</sup> Ga-(HE) <sub>3</sub> -Z <sub>HER3</sub> -NODAGA (3 h pi)	[ <sup>57</sup> Co]Co-(HE) <sub>3</sub> -Z <sub>HER3</sub> -DOTA (3 h pi)	[ <sup>57</sup> Co]Co-(HE) <sub>3</sub> -Z <sub>HER3</sub> -DOTA (24 h pi)	<sup>68</sup> Ga-(HE) <sub>3</sub> -Z <sub>HER3</sub> -NODAGA (3 h pi)	[ <sup>57</sup> Co]Co-(HE) <sub>3</sub> -Z <sub>HER3</sub> -DOTA (3 h pi)	[ <sup>57</sup> Co]Co-(HE) <sub>3</sub> -Z <sub>HER3</sub> -DOTA (24 h pi)
Blood	0.18 ± 0.01 <sup>a,b</sup>	0.33 ± 0.04	0.14 ± 0.02	12 ± 2 <sup>a</sup>	8 ± 1	18 ± 5
Salivary gland	0.7 ± 0.1 <sup>a</sup>	1.5 ± 0.1	0.9 ± 0.1	3.1 ± 0.6 <sup>a</sup>	1.9 ± 0.2	2.9 ± 0.6
Lung	0.81 ± 0.08 <sup>a</sup>	1.7 ± 0.2	0.6 ± 0.2	2.8 ± 0.3 <sup>a,b</sup>	1.6 ± 0.4	4.1 ± 0.9
Liver	2.2 ± 0.1 <sup>a,b</sup>	3.7 ± 0.5	1.6 ± 0.2	1.0 ± 0.1 <sup>a,b</sup>	0.74 ± 0.08	1.6 ± 0.3
Spleen	0.29 ± 0.04 <sup>a,b</sup>	0.43 ± 0.05	0.42 ± 0.08	8 ± 2	6 ± 1	6 ± 1
Stomach	0.8 ± 0.02 <sup>a,b</sup>	1.5 ± 0.3	0.65 ± 0.05	2.8 ± 0.6	2 ± 0.2 <sup>*</sup>	3.8 ± 0.9
Small Intestine	1.7 ± 0.04 <sup>a</sup>	4.6 ± 0.8	2.1 ± 0.04	1.3 ± 0.2 <sup>a</sup>	0.60 ± 0.05	1.3 ± 0.6
Kidneys	271 ± 36	253 ± 54	223 ± 23	0.008 ± 0.001	0.011 ± 0.002	0.011 ± 0.003
Tumor	2.3 ± 0.2	2.8 ± 0.4	2.4 ± 0.4	-	-	-
Muscle	0.10 ± 0.04 <sup>a</sup>	0.19 ± 0.01	0.09 ± 0.02	26 ± 12	15 ± 1	28 ± 4
Bone	0.3 ± 0.2	0.25 ± 0.06	0.20 ± 0.03	8 ± 5	11 ± 2	12 ± 3 <sup>e</sup>

Statistical significant differences ( $p < 0.05$ ) in uptake and tumor-to-organ ratios of [<sup>68</sup>Ga]Ga-(HE)<sub>3</sub>-Z<sub>HER3</sub>-NODAGA (3 h pi) and [<sup>57</sup>Co]Co-(HE)<sub>3</sub>-Z<sub>HER3</sub>-DOTA at <sup>a</sup> 3 h pi and <sup>b</sup> 24 h pi was determined with unpaired, two-tailed t-test.

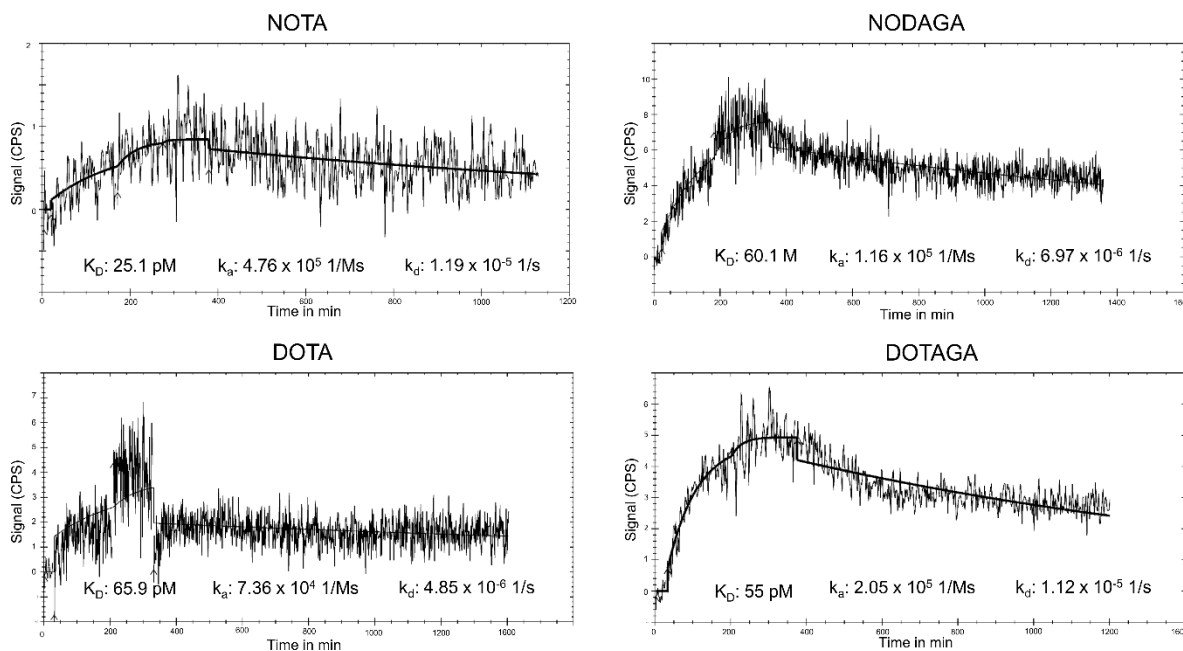


**Figure 1.** Representative Ligand Tracer Curves. Binding Kinetics of <sup>57</sup>Co-(HE)<sub>3</sub>-Z<sub>HER3</sub>-X were measured in real time on HER3 expressing BxPC-3 cells using Ligand Tracer yellow instruments (Ridgeview Instruments AB).

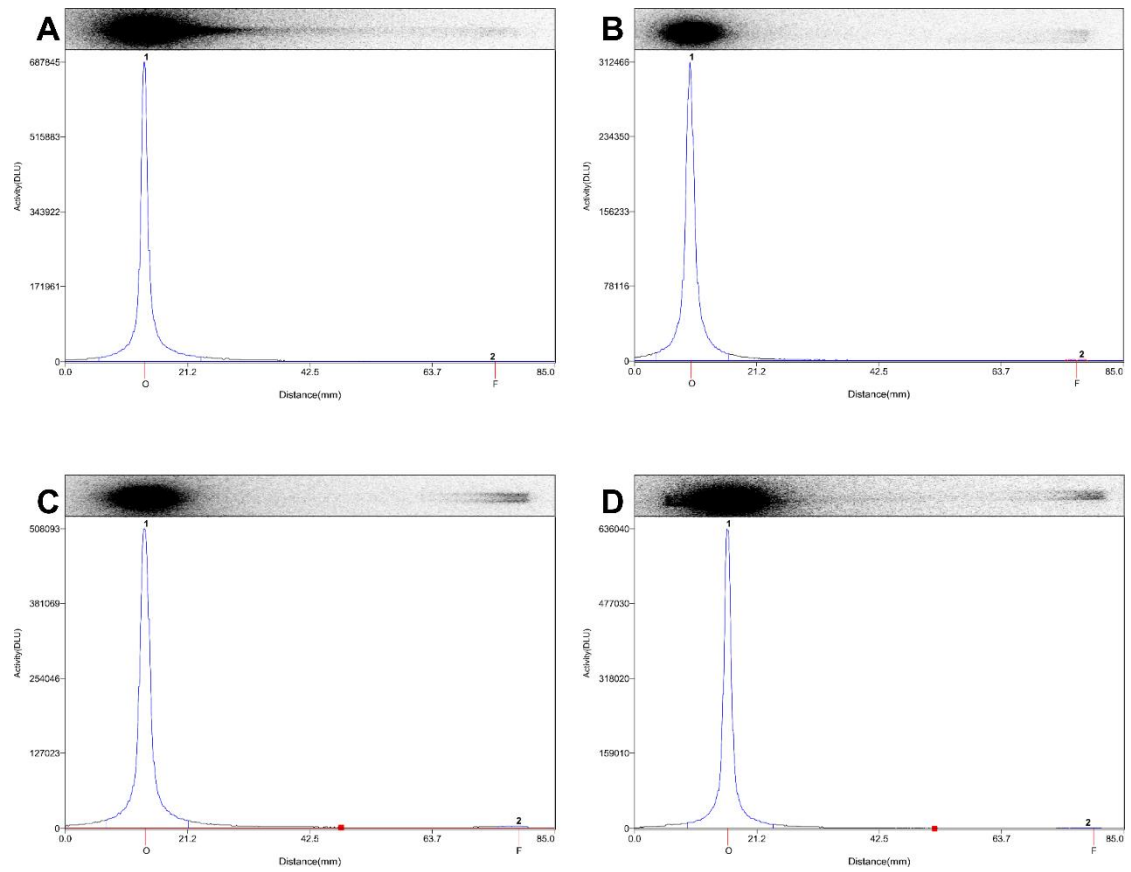


**Figure 2.** Representative ITLC traces of the radiolabeled products. (A)  $^{57}\text{Co}$ -(HE)<sub>3</sub>-Z<sub>HER3</sub>-NOTA (B)  $^{57}\text{Co}$ -(HE)<sub>3</sub>-Z<sub>HER3</sub>-NODAGA (C)  $^{57}\text{Co}$ -(HE)<sub>3</sub>-Z<sub>HER3</sub>-DOTA (D)  $^{57}\text{Co}$ -(HE)<sub>3</sub>-Z<sub>HER3</sub>-DOTAGA. Labeling was performed in ammonium acetate buffer (0.2 M, pH 5.5) for 45 minutes at 60 °C. Samples were taken from the labeling mixture and analyzed by ITLC using citric acid as the mobile phase. Radiolabeled conjugates remain at the application point (O) and free cobalt migrates to the front (F).